Burial of Organic Carbon in the Taiwan Strait

Weisen Liao[1,2] ID, **Jianfang Hu[1,3]** ID, **and Ping'an Peng[1,2]**

[1]State Key Laboratory of Organic Geochemistry, Guangzhou Institute of Geochemistry, Chinese Academy of Sciences, Guangzhou, China, [2]College of Earth and Planetary Sciences, University of Chinese Academy of Sciences, Beijing, China, [3]Key Laboratory of Ocean and Marginal Sea Geology, Chinese Academy of Sciences, Guangzhou, China

Abstract Organic carbon (OC) burial in nondeltaic continental shelves is an important part of the global carbon cycle. Of these, the Taiwan Strait (TWS) is a typical, nondeltaic shelf region that is influenced by a variety of factors including strong ocean currents, coastal upwelling, and small river inputs. To better understand how these factors influence OC burial in the TWS, we measured total organic carbon and total nitrogen contents as well as the stable carbon isotopes of sedimentary organic matter ($\delta^{13}C_{org}$) from the TWS. We also measured glycerol dialkyl glycerol tetraethers in surface sediments collected from the TWS. The concentrations of sedimentary total organic carbon and total nitrogen along the coast were high but decreased in areas more central to the TWS. This gradient was controlled by both hydrological conditions and coastal upwelling. The calculated accumulation rate of organic carbon ranged from 1.9 to 47.2 g C/m^2/year and was comparable to other areas of the Chinese marginal seas. The source contribution calculated from the three-end-member model revealed that mostly marine OC was buried in the upwelling regions. In comparison, OC derived from terrestrial plant and soil was buried in the estuaries. Collectively, these results showed that the TWS may serve as a CO_2 sink in the global carbon cycle. This is due to the preservation of the labile portions of the OC derived from plant and marine source, which formed the main component of the buried OC in the TWS.

Plain Language Summary Organic carbon (OC) burial in nondeltaic continental shelves is an important part of the global carbon cycle. Of these, the Taiwan Strait is a typical, nondeltaic shelf region that is influenced by a variety of factors including strong ocean currents, coastal upwelling, and small river inputs. This study addressed what control the distribution of OC and where different sources of OC (e.g., soil, plant, and marine) are buried. We demonstrated that the distribution of burial of OC was controlled by both hydrological conditions and coastal upwelling. Also, since the easily degradable marine OC formed the main component of the buried OC, we revealed that the Taiwan Strait may serve as a CO_2 sink in the global carbon cycle.

1. Introduction

Marine organic matter (OM) is the largest organic carbon (OC) pool on Earth, with approximately 80% of all global OC found buried in the Earth's continental shelves (Berner, 1982; Hedges & Keil, 1995). Because the accumulation of OM within these shallow areas plays a key role in the global carbon cycle, any change in its carbon pool may directly result in climate and/or environmental changes (Bauer et al., 2013). In order to evaluate the impact of carbon pool changes on the climate and environment, a quantitative assessment of OC located within continental shelves is necessary. Past work has been done toward this quantification; for instance, river delta and nondeltaic shelf regions bury an estimated 114 and 70 Tg C/year, respectively (Burdige, 2005). However, previous work has focused predominantly on large river deltas (e.g., Baudin et al., 2017; Feng et al., 2016; Galy et al., 2007; L. Hu et al., 2016; Sun et al., 2018; Yao et al., 2015), even though nondeltaic region covers a comparatively larger area. Critically, little is known about the carbon cycle in these spatially heterogeneous and dynamic environments, including how carbon is transported, remineralized, and buried (Zhu et al., 2011).

OC burial efficiency likely has significant variation across different continental shelves, owing to diverse depositional environments as well as changing hydrodynamic conditions, sedimentary rates, and bottom water oxygen concentrations (Allison et al., 2007; Bianchi & Allison, 2009). For instance, wide shelves (e.g., the Amazon shelf and the Yellow Sea) are characterized by low burial efficiency and are impacted mainly by marine processes (Aller & Blair, 2006; Feng et al., 2016). In comparison, small mountainous river shelves

(e.g., the U.S. West Coast) are characterized by high burial rates and impacted by both terrestrial and marine processes (Blair et al., 2003; Coppola et al., 2007; Feng et al., 2013; Goñi, Hatten, et al., 2013). Given these differences, a more thorough knowledge of the main controlling depositional environments will result in a better understanding of the size and spatial distribution of the OC pool.

Different OC sources—along with their different compositional properties and biological availabilities—have different respective contributions to the marine carbon pool and overall global carbon cycle (Bianchi et al., 2018; Blair & Aller, 2012; Galy et al., 2007). Generally, OM sources in marine carbon pools include terrestrial plants as well as soil- and marine-derived OM. More specifically, the burial of marine OC acts as an atmospheric CO_2 sink, while the delivery of terrestrial plants participates in marine biogeochemical processes (Blair & Aller, 2012; Drenzek et al., 2007; Feng et al., 2013). However, since soil OC is refractory and already part of the terrestrial carbon sink, soil OC burial in marine sediments is only a transportation from one carbon sink to another and has no influence on the atmospheric CO_2 content (Blair & Aller, 2012; Drenzek et al., 2007; Feng et al., 2013). Owing to the different diagenesis and transformation rates of different sources of OC, a better OC source analysis is needed.

Bulk organic parameters are typically used to track OM sources in continental shelf systems; such parameters include OC/N ratios and stable isotope ratios of elements in OM (e.g., Goñi, O'Connor, et al., 2013; J. Hu et al., 2006; Krishna et al., 2013; Wu et al., 2013). The marine and terrestrial OM OC/N ratios are generally ~5–8 and >15, respectively (Meyers, 1997). However, the absorption of inorganic nitrogen in clastic sediment can limit the use of OC/N ratios as a source indicator in marine sediments (Meyers, 1997). Furthermore, the use of stable carbon isotope ratios relies on an understanding of source signals. For example, the typical range of $\delta^{13}C$ values in terrestrial C_3 plants is −26 to −28‰, whereas the $\delta^{13}C$ values in marine phytoplankton range from −19 to −21.9‰ (Fry & Sherr, 1984; Meyers, 1997). However, the interpretation of such data can be further complicated by the possibility of multiple terrigenous sources of OM (Wu et al., 2013; Yao et al., 2015).

The limitations of these bulk geochemical approaches can be overcome by using specific biomarkers (Wu et al., 2015; Zhu et al., 2013). Recently, a biomarker ratio based on the relative abundance of glycerol dialkyl glycerol tetraethers (GDGTs) known as the branched/isoprenoid tetraether (BIT) index (Hopmans et al., 2004) was proposed for use in tracing terrestrial OC inputs—particularly those of soil OC to marine sediments (Smith et al., 2010). The BIT index is based on the relative contributions of GDGTs derived from soil bacteria (branched GDGTs or brGDGTs) and GDGTs from marine Thaumarchaeota (isoprenoid GDGTs or isoGDGTs; in this case, crenarchaeol; Hopmans et al., 2004). In soil, the BIT value is close to 1, while pure marine OM has a value close to 0 (Kim et al., 2006; Weijers et al., 2006). Given this range, the BIT index is a useful tool to assess the flux of OM in continental shelf systems that derives from soils (Kim et al., 2006; Walsh et al., 2008; Yao et al., 2015). Therefore, more specific sources (e.g., soil, plant, and marine OM) can be differentiated using a multiproxy method that combines the BIT index, C/N, and $\delta^{13}C$ (Smith et al., 2010; Weijers et al., 2009).

The Taiwan Strait (TWS) serves as connection between the South China Sea (SCS) and the East China Sea (ECS). Given its geographical location, it is a unique environment that is subjected to strong ocean currents, coastal upwelling, and massive terrestrial input. These factors form heterogeneous depositional conditions and produce different input sources for OC. Ultimately, this leads to differences in OC pools. Despite this heterogeneity, previous work has focused mostly on the carbon burial in the ECS (Deng et al., 2006; L. Hu et al., 2012, 2016; Li et al., 2013) rather than the TWS.

Given this lack of understanding of the TWS, the main goals of this study were twofold: (1) to explore the controlling factors behind the distribution of buried OC in the TWS and (2) to assess the source composition of buried OC and infer its influence in the carbon cycle. To do this, we investigated the TWS in terms of its spatial distribution of total organic carbon (TOC) and total nitrogen (TN), the values of stable carbon isotopes in its sedimentary OM, and the levels of GDGTs in its surface sediments. We then combined these results with the accumulation rate (AR) presented in Huh et al. (2011) to quantitatively estimate carbon burial in the TWS.

2. Materials and Methods

2.1. Study Area

The study area was located in the northern and western TWS, between 23.5–27°N latitude and 118.5–121°E longitude (Figure 1). More broadly, the TWS is located between Taiwan Island and the southeastern Chinese
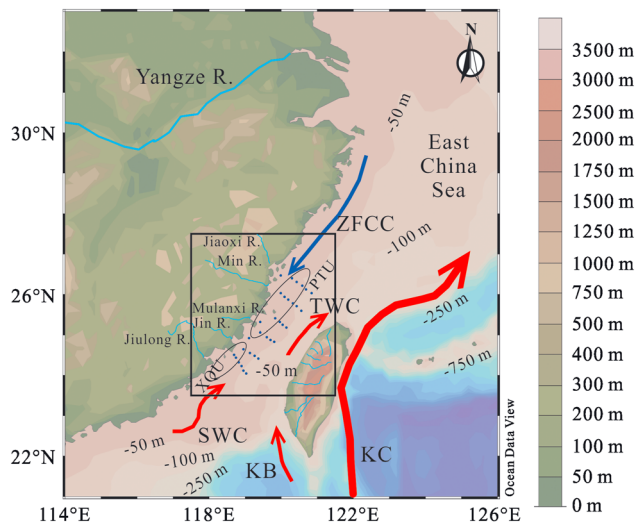
Figure 1. Map of the Taiwan Strait showing its topography and ocean currents. The solid, red, arrowed lines indicate warm currents flowing from the south, including the Kuroshio Current (KC), the Kuroshio branch (KB), the South China Sea Warm Current (SWC), and the Taiwan Warm Current (TWC). The solid, dark blue, arrowed line indicates the Zhejiang-Fujian Coastal Current (ZFCC) flowing from the north. The ellipses indicate the Xiamen-Quanzhou upwelling (XQU) and Pingtan upwelling (PTU) regions. The solid, light blue lines indicate rivers flowing into the Taiwan Strait. The locations of the sampling stations are denoted with blue dots. Note that this figure was created using Ocean Data View (Schlitzer, R., Ocean Data View, http://odv.awi.de, 2017).

mainland. It is approximately 180 km wide and 350 km long, with an average water depth of 60 m. Water circulation and the formation of upwelling regions in the TWS are driven by a complex bottom topography coupled with strong, seasonal monsoon forces (Gan et al., 2009; Hong et al., 2011; J. Hu et al., 2003; Liang et al., 2003). There are three major ocean currents in the TWS that control its hydrological conditions: the Zhejiang-Fujian Coastal Current (ZFCC), the Taiwan Warm Current (TWC), and the incursion of the Kuroshio Current branch. The ZFCC is the strongest during the winter, due to the influence of the East Asian Monsoon. The TWC and Kuroshio Current branch are both strongest during the summer (J. Hu et al., 2011; L. M. Hu et al., 2011; Qiu et al., 2011).

The upwelling regions in the TWS have been well defined by previous studies (J. Hu et al., 2001, 2003; Qiu et al., 2011). Of these, the Xiamen-Quanzhou upwelling and the Pingtan upwelling (PTU) regions are the most important. They are both wind-driven, topographically forced coastal upwelling systems, which form in the western TWS during the summer monsoon period (Tang et al., 2002).

There are many small rivers around the TWS, eight of which are greater than 100 km in length (Chen et al., 1998; Milliman & Farnsworth, 2011). These include the Min, Jiulong, Jin, Jiaoxi, and Mulanxi Rivers, which flow into the TWS from mainland China. The Tanshui, Tachia, and Choshui Rivers flow into the TWS from Taiwan Island. Collectively, these rivers discharge 87 Mt of sediment annually into the TWS and are large sources of terrestrial OC (Chen et al., 1998; Milliman & Farnsworth, 2011).

2.2. Sampling Sites and Procedure

The study area covered the northern and western TWS and was influenced by previously described ocean currents, coastal upwelling regions, and terrestrial inputs. It consisted of six land-ocean sections, with each section consisting of four to six sampling sites (Figure 1). In addition, three sampling locations were located at major river estuaries (the Jin, Mulanxi, Jiaoxi, and Min Rivers). A total of 32 surface sediment (0–5 cm) samples were collected with a stainless-steel grab sampler onboard the R/V YANPING II in July 2016. All samples were packed into presterilized aluminum foil in polyethylene bags and stored at −20 °C until further analysis.

2.3. Grain-Size Analysis

Approximately 1 g of each freeze-dried sample was used for grain-size analysis. Briefly, samples were pretreated with 10% H_2O_2 and 1 N HCl to remove all OM and dissolvable salts. The pH of the resulting solution from the residual sample was adjusted to 7 by repeatedly rinsing the samples with distilled water. A 0.05 N $(NaPO_3)_6$ solution was then added to disperse any particles. Sample grain sizes were measured using a Malvern Mastersizer 2000G laser diffraction particle analyzer with ultrasonic pretreatment. The measurement range was 0.02–2,000 μm with a relative error of less than 2%.

2.4. Elemental and Stable Carbon Isotope Analyses

The remaining sediment samples were freeze dried, homogenized, and ground into powder. Individual samples were then subdivided for TOC, TN, and isotope analyses. Briefly, these samples were treated with 6 N HCl for 24 hr to remove any carbonate, then rinsed with deionized water. The carbonate-free samples were dried, then analyzed for OC and TN content using a Thermo Fisher Scientific FLASH EA 1200 Series CNS elemental analyzer. Every sample was run in duplicate and the means were used for all analysis. Replicate analysis of one sample ($n = 5$) gave a 1σ precision of ±0.02 wt %C and ±0.003 wt %N.

All $\delta^{13}C_{org}$ analyses were performed on carbonate-free sediment samples using a FLASH2000 Elemental Analyzer connected to a Thermo MAT-253 isotope ratio mass spectrometer. Results are reported using standard delta notation in permil units (‰) according to the following equation:

$$\delta\ (‰) = \left(R_{\text{sample}} - R_{\text{reference}}\right)/R_{\text{reference}} \times 1,000$$

where $\delta\ (‰)$ is $\delta^{13}C\ (‰)$ and R_{sample} and $R_{\text{reference}}$ are the isotopic ratios of the sample and reference materials, respectively. The reference standard used was Peedee belemnite. Analytical precision for international and in-house reference materials was largely better than $\pm 0.2‰$ ($n = 5$). Replicate measurements of samples yielded similar standard deviations.

2.5. Glycerol Dialkyl Glycerol Tetraethers

A total of 30 g of each powdered sample was spiked with an appropriate amount of C_{46}-GDGT standard compound, then extracted via Soxhlet reflux for 72 hr using a mixture of dichloromethane (DCM) and methanol (9:1, vol/vol). The resulting mixture was centrifuged, and the organic phase was separated from the aqueous phase using a separation funnel following the addition of a 5% solution of KCl. The aqueous phase was extracted with DCM (3 times using 15 ml), and the collected organic material was concentrated by rotary evaporation. The total lipid extract was saponified with 6% KOH, and the neutral fraction was extracted using hexane. The neutral fraction was then separated into nonpolar and polar fractions on an active silica gel column by elution with a hexane/DCM mixture (9:1, vol/vol) and a DCM/methanol (1:1, vol/vol), respectively. The polar fraction (DCM/methanol) was condensed by rotary evaporation, redissolved in a hexane/ethyl acetate (EtOAc) mixture (84:16, vol/vol), and filtered through a 0.45-μm polytetrafluoroethene filter prior to analysis.

High-performance liquid chromatography/atmospheric pressure chemical ionization-mass spectrometer (HPLC/APCI-MS) was used to analyze the GDGT content of all samples. Analyses were performed using a Thermo Accela HPLC system liquid chromatograph and a Thermo TSQ Vantage triple quadruple mass spectrometry, equipped with an autoinjector. Samples (10 μl) were injected, and separation of 5- and 6-methyl brGDGTs was achieved with two silica columns in tandem (150 mm $\times$ 2.1 mm, 1.9 μm; Thermo Finigan; USA) maintained at 40 °C. The eluent gradient was modified from Yang et al. (2015). Briefly, GDGTs were eluted isocratically for the first 5 min with 84% A and 16% B, where A = n-hexane and B = EtOAc. The following elution gradient was used: 84/16 A/B to 82/18 A/B for 5–65 min, 100% B for 21 min, 100% B for 4 min to wash the column, and then 84/16 A/B to equilibrate the column for 35 min at a constant throughput of 0.2 ml/min. GDGTs were detected using selected ion monitoring mode, following the methods described in Schouten et al. (2007). The MS conditions were followed according to those published by Pearson et al. (2011). Integration of the peak area of the $[M + H]^+$ ion traces was used to quantify all GDGT content. Each sample was analyzed in duplicate, and the data presented are mean values. Replicate HPLC/APCI-MS analysis of one sample revealed the reproducibility of the BIT index to be ± 0.035. Indices based on the distribution of GDGTs were calculated following Hopmans et al. (2004) and the following ratio:

$$BIT = \frac{Ia + IIa + IIa' + IIIa + IIIa'}{\left(Ia + IIa + IIa' + IIIa + IIIa' + Cren.\right)}$$

2.6. Statistical Analyses

Statistical significance was determined using Pearson correlation analyses and two-tailed Student's t tests. All analyses were performed using SPSS 22.0. Origin 9.0 data analysis and graphic software was used for all graphs. Maps showing the spatial distribution of the surface sediment parameters from the TWS were produced using the DIVA method in Ocean Data View (Schlitzer, R., Ocean Data View, http://odv.awi.de, 2017).

3. Results

3.1. Bulk Sediment Properties

The grain size composition of sediments from the TWS was divided into three groups based on grain size: clay (<4 μm), silt (4–63 μm), and sand (>63 μm). The relative percent of clay, silt, and sand content in total particles ranged from 0 to 21.0%, 0 to 84.1%, and 1.1 to 100%, respectively. We defined the sum of clay and silt as fine-grained sediments; their collective content ranged from 0 to 98.9%. The spatial distribution of fine-grained sediments of the TWS is presented in Figure 2a. The northern and western TWS sediments were dominated by fine-grained sediment, with a relative content of 56.9–98.9%. Comparatively, central TWS sediments were dominated by coarser grain sediments, as their fine-grained sediment content only ranged from 0 to 47.6%. Notably, fine-grained sediment content decreased across the TWS from west to east and from north to south.
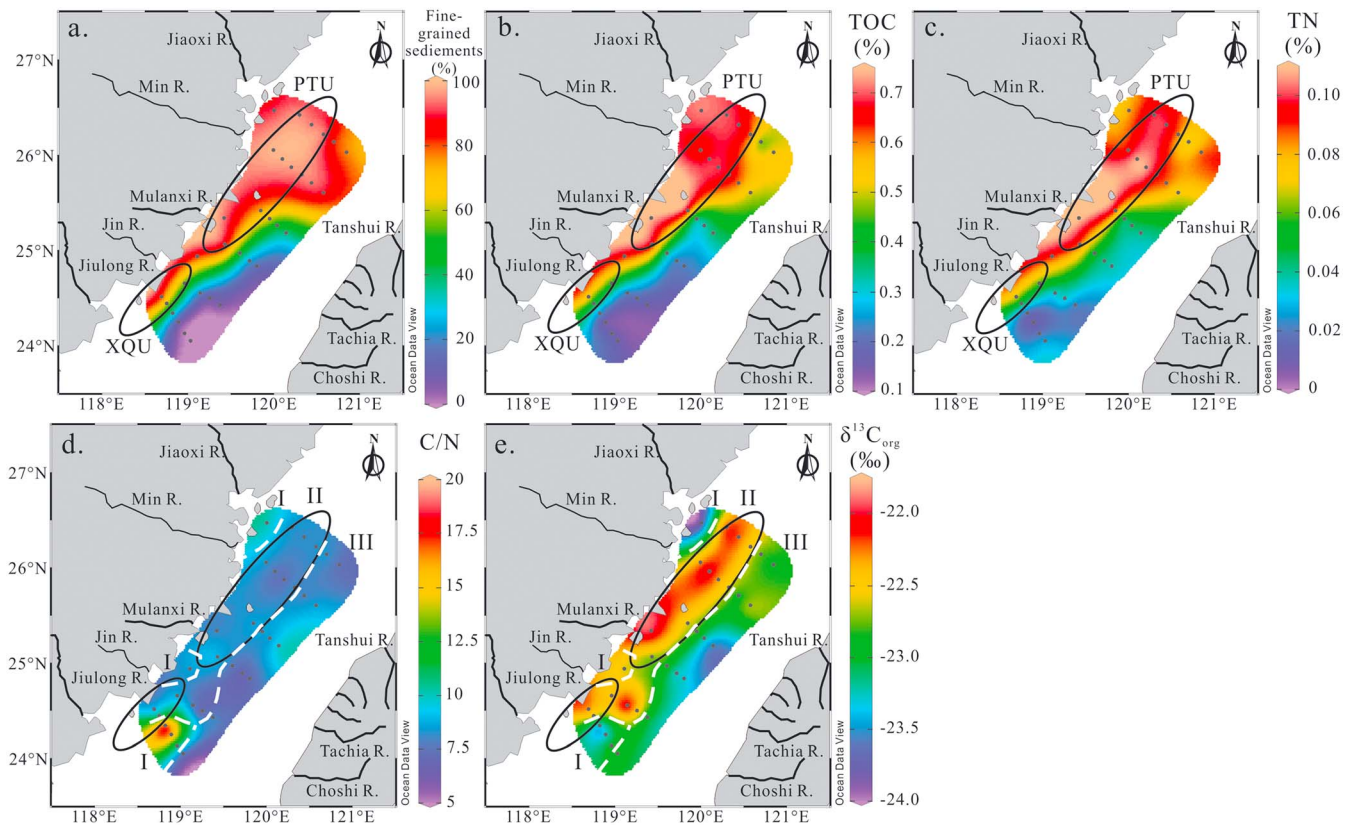
Figure 2. The spatial distribution of (a) fine-grained sediment, (b) total organic carbon (TOC) content, (c) total nitrogen (TN) content, (d) C/N atomic ratios, and (e) $\delta^{13}C_{org}$ in surface sediments of the Taiwan Strait. The ellipses indicate the Xiamen-Quanzhou upwelling (XQU) and Pingtan upwelling (PTU) regions. The white dashed lines indicate the regions defined in section 4.2.

Across the full sample set, TOC content ranged from 0.13 to 0.73%. TOC ranged from 0.25 to 0.73% in the northern and western areas of the TWS and from 0.13 to 0.36% in the central areas of the TWS (Figure 2b). The highest TOC content was found in the western TWS, close to Pingtan Island and within the PTU. The TOC content in the sediment along the coast was generally high but decreased toward the central areas of the TWS (Figure 2b). We also found a significant, exponential relationship between fine-grained sediment and TOC content ($r^2 = 0.901$, $p < 0.05$; Figure 3a).

As with TOC content, TN content was relatively high in the northern and western TWS and lower in the central TWS (Figure 2c). TN ranged from 0.01 to 0.11% in the full sample set, with the highest values seen in the western part of the TWS (Figure 2c). TN content ranged from 0.01 to 0.05% in the central TWS and increased toward the western and northern areas (Figure 2c).

There was a linear relationship between TOC and TN (Figure 3b), with the following regression equation: TOC% = 6.61, TN% + 0.04 ($r^2 = 0.937$, $p < 0.001$, $n = 32$). The regression line almost crossed the origin, suggesting that most of the nitrogen was related to sedimentary OC and therefore probably in an organic form (Figure 3b; Goñi et al., 1998; Hedges et al., 1986). In the full TWS sample set, the C/N atomic ratio ranged from 6.6 to 19.7 (Figure 2d). There was no obvious C/N ratio trend from the western or northern areas to the central areas of the TWS. More specifically, the ratio ranged from 6 to 10 in the TWS. There were only a few exceptions, including three samples obtained from the southern area of the TWS (C/N atomic ratios ranged from 10.3 to 19.7) and one sample from the Min River estuary (C/N ratio of 10.3).

The range of $\delta^{13}C_{org}$ values from the complete sample set ranged from −23.9 to −21.9‰ (Figure 2e). The most negative value (−23.9‰) was found in a sample obtained in close proximity to the Jiaoxi and Min River's estuaries. The $\delta^{13}C_{org}$ values were relatively negative along the coast as well as in the central areas of the TWS (Figure 2e). Finally, $\delta^{13}C_{org}$ values were less negative in the upwelling systems of the TWS (Figure 2e).
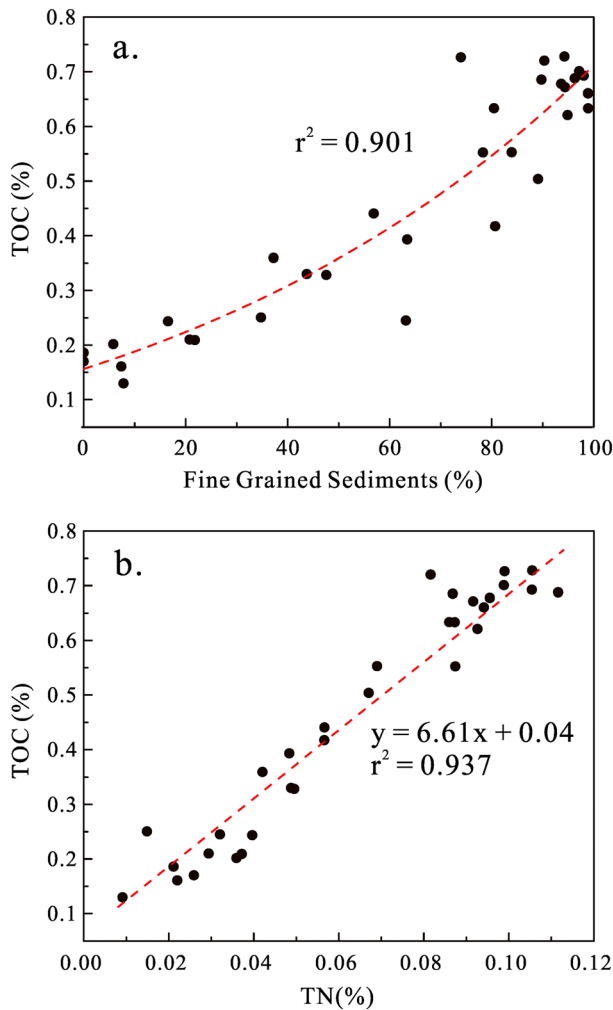
Figure 3. Correlation between (a) total organic carbon (TOC) content and fine-grained sediment and (b) TOC content and total nitrogen (TN) in surface sediments of the Taiwan Strait.

3.2. Branched GDGTs and BIT Index

brGDGT content from sediment samples ranged from 23.61 to 226.36 ng/g dry weight and the brGDGT content normalized to TOC ranges from 3.73 to 36.66 μg/g TOC (Figure 4a). This accounted for 4.1–15.5% of total GDGTs. The brGDGT fraction was dominated by GDGT-I compounds (i.e., GDGT-Ia, Ib, and Ic, accounting for 49–67% of total brGDGTs) and GDGT-II (27–41% of total brGDGTs). The brGDGT content normalized to TOC was relatively high in the southwestern and northeastern areas of the TWS. The distribution of the percentage of total brGDGTs was similar to the brGDGT content normalized to TOC, with the exception of the northeastern area of the TWS. In most samples, brGDGT content was below 10% of total GDGTs, with the exception of four samples near the river mouths of both the Jiulong and Jin Rivers.

The BIT index from the full set of sediment samples ranged from 0.04 to 0.17 (Figure 4b). The BIT index ranged from 0.04 to 0.17 in the central areas of the TWS and 0.04 to 0.16 in the northern and western areas of the TWS. The highest BIT index values occurred in the southern and western areas of the TWS, which were located near the Jiulong and Jin Rivers' estuaries (Figure 4b). The BIT index was also slightly increased at the Jiaoxi and Min River's estuaries.

4. Discussion

4.1. Spatial Distribution of Buried OC

It is known that the bulk OC in continental shelves is closely associated with fine-grain particle sizes (Bianchi et al., 2018; Hedges & Keil, 1995). In the TWS, the TOC contents showed a significant, exponential correlation with the relative proportion of fine-grained sediment. The flattening of TOC content in areas of that have low fine-grained sediment proportions has also been observed in other shelf sediments (e.g., J. Hu et al., 2006; L. Hu et al., 2012; Ramaswamy et al., 2008). In the ECS, initially deposited sediments are readily resuspended and transported southward along the coast, driven by the wind-induced waves in the winter and by the ZFCC. This results in the formation of a muddy belt along the coast (Bian et al., 2013; L. M. Hu et al., 2011; Liu et al., 2006, 2007). Since the
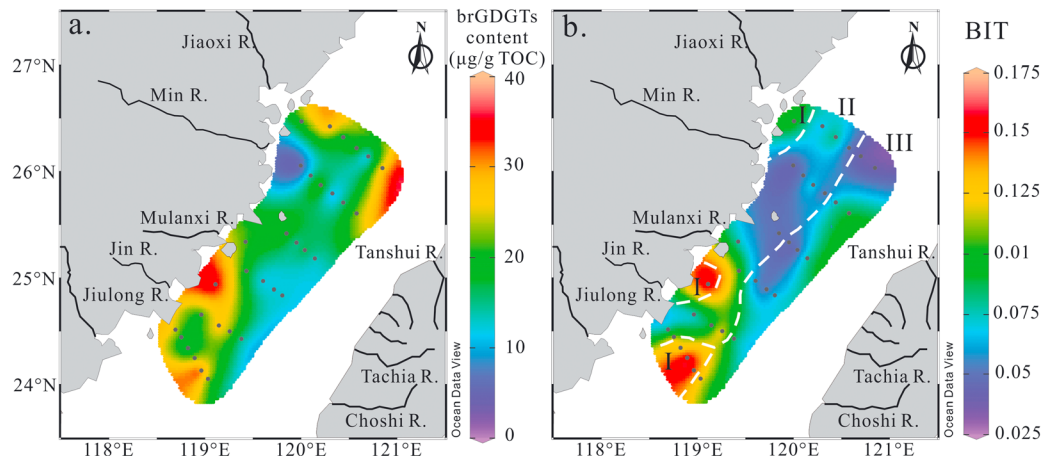

Figure 4. Spatial variation in (a) total organic carbon (TOC)-normalized branched glycerol dialkyl glycerol tetraether (brGDGT) contents and (b) branched/isoprenoid tetraether (BIT) index in surface sediments of the Taiwan Strait.
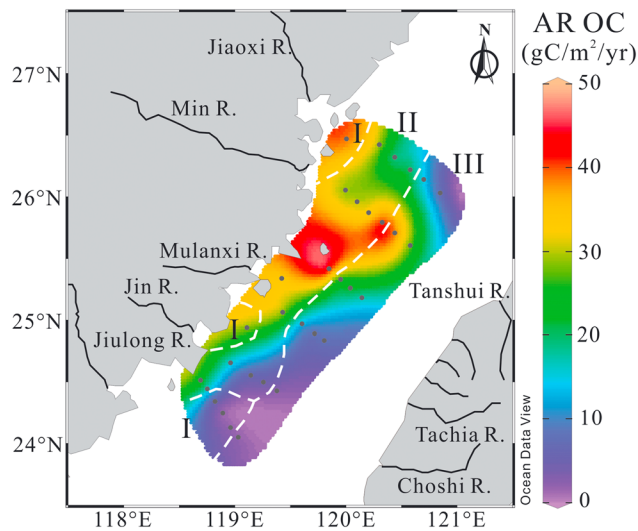
Figure 5. Spatial variation in the accumulation rate of total organic carbon (AROC) in surface sediments of the Taiwan Strait.

ZFCC weakens as it travels southward, the proportion of fine-grained sediment decreased in more southern areas. Given this, the spatial distribution of OC in the TWS is controlled by its specific hydrological conditions, which is corroborated by observations from other continental shelves around the world (e.g., Galy et al., 2007; L. Hu et al., 2012; Ramaswamy et al., 2008).

Upwelling of cold and nutrient-rich water along the coast in the summer is another major oceanographic feature of the TWS (Hu & Wang, 2016). Satellite-derived chlorophyll *a* concentrations display a distinct seasonality, with maxima between June and September each year (Shang et al., 2004). Past work has revealed a statistically significant, negative linear relationship between SST and chlorophyll *a*, indicating that the coastal TWS productivity is primarily controlled by the upwelling (J. Hu et al., 2001; Hu & Wang, 2016). This high primary production induces POC flux (Sun et al., 2012; Wang et al., 2017). Moreover, TOC contents in the PTU are consistent with the POC contents of descending particles (Wang et al., 2017). Correlating with our data, it can be inferred that upwelling-related, high primary productivity may cause the increase of OC and N contents observed in coastal surface sediments.

Huh et al. (2011) conducted a comprehensive study of the AR of bulk sediment in the TWS. We calculated the AR of organic carbon (AROC) based on the AR determined by Huh et al. (2011). The ARs were taken from the contour map of AR presented in Huh et al. (2011), which covered more than 50 data points in our study area. Using these sedimentation rates, the AR of sedimentary OM was calculated as follows:

$$AROC\ (accumulation\ rate\ of\ organic\ carbon) = AR \times TOC$$

The calculated AROC ranged from 1.9 to 47.2 g C/m^2/year. The AROC spatial distribution in the TWS revealed enhanced OC burial in the western areas of the TWS with greater importance of the PTU; this distribution decreased from the west to the east (Figure 5).

Spatially, TOC ARs exhibited a broad range across the TWS, with several patches of high TOC depositional flux (Figure 5). The highest TOC AR was more than 45 g C/m^2/year and was observed near the Pingtan Island. Relatively high OC ARs of more than 40 g C/m^2/year were also observed to the northeast of Pingtan Island, within the region affected by the PTU. Another subregion with relatively high TOC depositional flux was observed in the Jiaoxi and Min River's estuaries. This observation is likely explained by its high flux of sediment accumulation.

Average TOC sequestration rates were estimated on a TWS regional scale to be 20.1 g C/m^2/year. If we only focus on the northern and western areas of the TWS, this average sedimentary OC sequestration rate increases to 27.6 g C/m^2/year. This is notably higher than the global average of coastal OC burial rates (~4 g C/m^2/year; Berner, 1982). Together, a total mass budget of sedimentary TOC of 0.44 × 10^6 t C/year was obtained for the sampled region (~22,000 km^2; Figure 5). The TOC accumulation and sequestration rates in the TWS were comparable to those of other coastal margins in the world that had significant river discharge and/or high primary production (Table 1). These include areas like the Bohai Sea (27 g C/m^2/year; L. Hu et al., 2016), the Louisiana Inner Shelf (22.7 g C/m^2/year; Gordon et al., 2001), the Amazon Shelf (58.2 g C/m^2/year; Aller et al., 1996), and the North Sea (35 g C/m^2/year; de Haas & van Weering, 1997). TOC accumulation and sequestration rates were even higher than other marginal seas in China, such as the Yellow Sea (15.3 g C/m^2/year; L. Hu et al., 2016) and the ECS (Deng et al., 2006). This comparison suggests that the TWS likely serves as a significant, global repository of sedimentary OC.

4.2. Characterization of Sources for Buried OC

Based on our C/N, $\delta^{13}C_{org}$, and BIT ratios, we divided our study area into three subregions (Figure 2): Region I was close to the river estuary and was characterized by high C/N ratios (8.6–19.7), negative $\delta^{13}C_{org}$ values (−22.6 to −23.9‰), and a high BIT index (0.11–0.17). Region II was inside the upwelling systems and was

Table 1

Comparison of TOC Burial Rates and Mass Budget in Global Coastal Margins

Shelf	Area (10^6 km^2)	TOC burial rates (g/m^2/yr)	TOC budget (Mt/year)	Reference
Amazon Shelf	–	58.2	–	Aller et al. (1996)
Northeastern North Sea	–	35	–	de Haas et al. (1997)
Louisiana inner shelf	–	22.7	0.18	Gordon et al. (2001)
East China Sea	0.5	14.7	7.4	Deng et al. (2006)
Bohai and Yellow seas	0.36	15.3 (0.03–746.9)	5.6	L. Hu et al. (2016)
Bohai Sea	0.074	27	2	L. Hu et al. (2016)
Taiwan Strait	0.022	20.1	0.44	This study
Global shelves	26	4.15	108	Berner (1982)

characterized by low C/N ratios (6.6–9.5), less negative $\delta^{13}C_{org}$ (−21.9 to −22.8‰), and a low BIT index (0.04–0.14). Region II was also dominated by high TOC content (average 0.58%) and fine-grained sediment (average 77.7%). Region III was in the central area of the TWS and was generally characterized by low C/N ratios (6.6–10.0), a low BIT index (0.04–0.12), and negative $\delta^{13}C_{org}$ (−22.6 to −23.6‰). Region III also had depletion of ^{13}C and an increasing BIT index toward the east.

Bulk sedimentary OC was divided into marine and terrestrial components. The C/N ratio of degraded marine phytoplankton approximated 6–7, while vascular plants are nitrogen-depleted and have C/N ratios greater than 20 (Hedges & Oades, 1997; Meyers, 1994). In the TWS, C/N ratios generally varied between 6 and 10, suggesting a mixture of marine and terrestrial OM (Figure 2d). The highest observed C/N ratio (19.7) occurred in the southern—not coastal—TWS (Figure 2d), indicating a more significant influence of the Jiulong River. Even though there are no data between the Jiulong River and this region, previous work also supports this conclusion, as the Jiulong River plume has been shown to reach the sample location at high flux (Lin et al., 2016; Wang et al., 2013). Moreover, the C/N ratios were the highest in Region I, indicating a notable terrestrial input in this heavily river-influenced region.

Measured $\delta^{13}C_{org}$ values in the TWS ranged from −21.9 to −23.9‰. This range overlaps with those seen in terrestrial C$_3$ plants (−33 to −22‰; Bender, 1971) and marine phytoplankton (−23 to −17 ‰; Bouillon et al., 2008), indicating that OM derived from both marine and terrestrial sources is present in the sampled TWS sediments (Figure 2e). As shown in Figure 2e, the $\delta^{13}C_{org}$ values were the most positive in Region II. As previously mentioned, this region was in the upwelling region with high primary productivity. The marine phytoplankton blooms found there supply the marine OC, resulting in enriched $^{13}C_{org}$. The $\delta^{13}C_{org}$ was relative negative in Region I, especially in sampled areas influenced by the Jiaoxi and Min Rivers (−23.9‰) as well as the Jiulong River (average −23.3‰). In Region III, $\delta^{13}C_{org}$ was more negative in eastern samples, suggesting the influence of Taiwanese mountain rivers reaching the middle of the TWS. There are many mountain rivers in the island of Taiwan that have high erosion rates (Kao et al., 2008). However, sediments from most of these rivers are transported for only a short distance (Kao et al., 2008, 2014), with the strong currents of the TWC carrying these sediments northward into the ECS (Horng & Huh, 2011; Huh et al., 2011). Therefore, the influence of Taiwanese mountain rivers is constrained to the central areas of the TWS.

The BIT index is based on the relative abundance of branched GDGTs and crenarchaeol, representing the relative contribution of terrestrial OM (Hopmans et al., 2004). Our data revealed that BIT index values were higher in Region I—given the influence of terrestrial river input—and lowest in Region II. As with $\delta^{13}C_{org}$ values, BIT values from Region III increased steadily toward the middle of TWS. This also suggested the limited influence of Taiwanese mountain rivers. Taken together, these results indicate that terrestrial OM is predominantly deposited under the direct influence of terrestrial input.

Recent evidence has shown that the covariation of crenarchaeol and brGDGTs in sediments may be the result of in situ brGDGT production (Fietz et al., 2012; Xing et al., 2016). Moreover, as the index is a ratio, its value may depend on in situ aquatic crenarchaeol production and not be representative of variations in terrestrial inputs (Fietz et al., 2011). However, our correlation analyses revealed $r^2 = 0.13$ for the relationship between the BIT index and crenarchaeol and $r^2 = 0.27$ for that between the BIT index and brGDGTs. These findings suggest that aquatic Thaumarchaeota variation is not the controlling factor for BIT values. Furthermore,

there was no relationship between crenarchaeol and brGDGTs ($r^2 = 0.21$), suggesting that crenarchaeol and brGDGTs originated from different sources. Therefore, it is possible to use the BIT index to trace terrestrial input.

Some studies have shown that the BIT index is linearly correlated with $\delta^{13}C_{org}$ values (Smith et al., 2010, 2012); others have shown only a weak or no significant correlation (e.g., Walsh et al., 2008; Xing et al., 2014). The correlation between the BIT index and $\delta^{13}C_{org}$ has been attributed to the relative importance of soil- and plant-derived OC input (Smith et al., 2010). As we found no evidence for a relationship between $\delta^{13}C_{org}$ and BIT ($r^2 = 0.04$), it is possible that the terrestrial input includes more than one source. Given this, a three-end-member model would be needed to distinguish individual OM sources.

4.3. Source Influences on Buried OC

It has been increasingly recognized in the literature the need to define soil OM as a distinct OC source in end-member mixing models (e.g., Bianchi et al., 2002; Goñi et al., 2006; Schreiner et al., 2013; Weijers et al., 2009; Xing et al., 2014). Here we have the possibility of tracing the relative contribution of soil OC by means of the BIT index, which is a proxy for fluvial input of soil OM. We used the BIT index data in conjunction with the $\delta^{13}C_{org}$ of the OM in a three-end-member model, similar to that described by Weijers et al. (2009). This approach would thus allow us to separate the terrestrial OC fraction into both a soil and plant OC fraction. As the BIT index can trace soil OC and the $\delta^{13}C_{org}$ can distinguish between plant- and soil-derived OC, these three parameters were used.

As such, the two equations on which the three-end-member mixing model was based are as follows:

$$BIT_{Sample} = (BIT_{Mar} \times f_{Mar}) + (BIT_{Soil} \times f_{Soil})$$
$$\delta^{13}C_{Sample} = \left(\delta^{13}C_{Mar} \times f_{Mar}\right) + \left(\delta^{13}C_{Soil} \times f_{Soil}\right) + \left(\delta^{13}C_{Plant} \times f_{Plant}\right)$$

With the additional mass balance equation of

$$f_{Mar} + f_{Soil} + f_{Plant} = 1$$

f_{Mar}, f_{Soil}, and f_{Plant} are the fractions of marine, soil, and plant OC, respectively.

The end-members used to characterize marine OM were assumed to be 0.04 for BIT and −20.0‰ for $\delta^{13}C$ (Hedges & Oades, 1997). With respect to soil, the end-member value was 0.91 for BIT_{soil} (Weijers et al., 2006) and −24.6‰ for $\delta^{13}C_{Soil}$. As previously published, this value is the average soil value along the main channel of the Yangtze River (Wu et al., 2007). By referencing prior research results for the Yangtze River estuary and ECS shelf (B. Hu et al., 2014; Zhang et al., 2007), this paper assumed a value of −28.7‰ for $\delta^{13}C_{Plant}$. Since plant debris contains little brGDGTs, the BIT_{Plant} was assumed to be 0.

The estimated f_{Mar}, f_{Soil}, and f_{Plant} ranged from 1.2 to 15.8%, 18.9 to 40.1%, and 50.8 to 76.3%, respectively. The spatial distribution for f_{Mar}, f_{Soil}, and f_{Plant} are shown in Figures 6a–6c. The soil component was the smallest in the TWS, with the highest values located in Region I. This implies that the river input is the main source of terrestrial soil. The plant component was the largest terrestrial component, consisting of a larger fraction in the central TWS and Min River estuary.

However, it has been shown that preaged OC—especially petrogenic OC with $\Delta^{14}C_{org}$ approximating 1000‰ is an important source of terrestrial OC in marine sediments (Bao et al., 2016; Bianchi et al., 2018; Tao et al., 2015). Bao et al. (2016) studied the $\Delta^{14}C_{org}$ of the TWS, and its distribution is shown in Figure 7. In the central TWS, the relatively low $\Delta^{14}C_{org}$ indicates the input of petrogenic OC from the island of Taiwan (Bao et al., 2016). Since the average $\delta^{13}C_{org}$ of Taiwanese rivers is −25.2‰ (Hilton et al., 2010), the fraction of OC_{plant} may be overestimated because petrogenic OC can also cause the depletion of $^{13}C_{org}$. Bao et al. (2016) showed that the $\Delta^{14}C_{org}$ for the rest of TWS was generally −250 to −350‰ and was not caused by petrogenic OC. Instead, the general depletion of $^{14}C_{org}$ in the TWS is caused by the resuspension-deposition loops during which the OM aged (Bao et al., 2016). This conclusion is supported by the observation that 65–85% of settling particulate matter originate from the resuspension of bottom sediments (Wang et al., 2017). Therefore, the three-end-member model using soil, plant, and marine OM can still be applied to the rest of the TWS, with the exception of the central areas of the TWS that are influenced by Taiwanese river inputs.
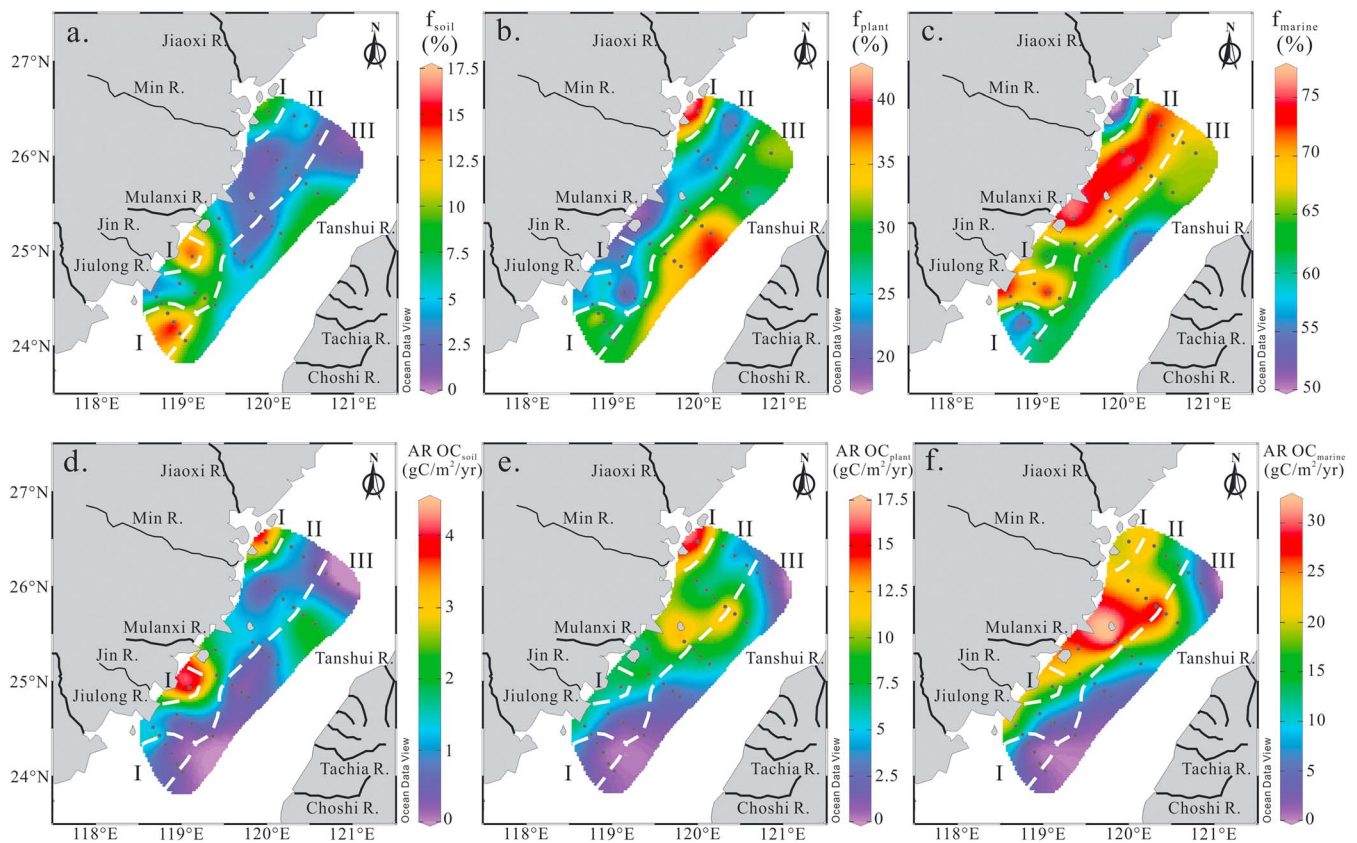
Figure 6. Spatial variation in (a) relative fraction of soil-derived organic carbon (f_{soil}), (b) relative fraction of plant-derived organic carbon (f_{plant}), (c) relative fraction of marine-derived organic carbon (f_{marine}), (d) accumulation rate of soil-derived organic carbon (AROC$_{soil}$), (e) accumulation rate of plant-derived organic carbon (AROC$_{plant}$), and (f) accumulation rate of marine-derived organic carbon (AROC$_{marine}$), in surface sediments of the Taiwan Strait.

Figure 7. Spatial variation of $\Delta^{14}C_{org}$ (‰) in surface sediments of the Taiwan Strait (adapted from Bao et al., 2016).

These source variations may have individually different influences on the buried OC. The erosion and burial of photosynthetically derived OC are a sink for atmospheric CO_2 (Bianchi et al., 2018; Stallard, 1998). In contrast, reburial of petrogenic OC from sedimentary rock is not a sink for atmospheric CO_2, since burial of the petrogenic OC is a simple recycling of reduced C and has no effect on the long-term atmospheric CO_2 and O_2 levels. In the TWS, most of the buried OC was photosynthetically derived; it may therefore serve as a sink for atmospheric CO_2.

To improve estimates of buried OC in the TWS, we quantified the relative proportion of soil, plant, and marine OC in the total OC pool. This has important implications for understanding global coastal carbon budgets (Cui et al., 2017). The AR of each source was calculated as follows:

$$\text{AROC}_x \text{ (accumulation rate of } x) = \text{AR} \times \text{TOC} \times f_x$$

where x represents the sources of OC, including soil, plant, and marine.

The calculated AROC$_{soil}$, AROC$_{plant}$, and AROC$_{marine}$ ranged from 0.1 to 4.1, 0.6 to 15.9, and 1.1 to 32.4 g C/m^2/year, respectively. The AROC$_{soil}$, AROC$_{plant}$, and AROC$_{marine}$ spatial distributions in the TWS indicated that enhanced OC burial occurred along the coast, while marine OC accumulated primarily in the PTU regions (Figures 6d–6f). However, soil OC and plant OC were mainly deposited at the Jin and Min Rivers' estuaries, respectively. In the central TWS, even though the terrestrial input fraction from Taiwan Island was high, the AROC$_{plant}$ was low due to the low AR.

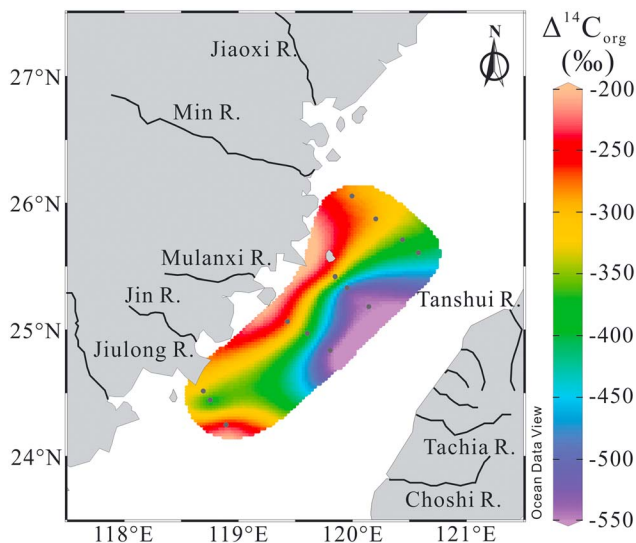Nevertheless, these findings suggest that OC burial in the TWS was mainly marine-derived OC and that it was mostly deposited in the upwelling area. Comparatively, the plant- and soil-derived OC were mainly buried along the coast. These findings have important implications for OC burial in subtropical, nondeltaic continental shelves under the influences of strong ocean current, coastal upwelling, and small mountain rivers.

5. Conclusions

The TOC and TN contents as well as the grain size of 32 surface sediments were measured to better understand the size and spatial distribution of buried carbon in the TWS. A three-end-member model was used to estimate the source contribution of soil, plant, and marine components based on both the $\delta^{13}C_{org}$ and BIT index. Our results showed that the spatial distribution of OC in the TWS was controlled by the hydrological conditions and coastal upwelling. The total buried carbon budget may be up to 0.44×10^6 t C/year, and comparisons to other continental shelves suggested that the TWS likely serves as a significant repository for global sedimentary TOC. The marine-derived OC was mainly deposited in the upwelling regions, while the plant-derived OC was mainly deposited in the river-influenced regions. The burial of predominantly fresh components (marine and plant) of OC imply that the TWS functions as a carbon sink for the global carbon cycle.

References

Aller, R. C., & Blair, N. E. (2006). Carbon remineralization in the Amazon-Guianas tropical mobile mudbelt: A sedimentary incinerator. *Continental Shelf Research*, *26*(17–18), 2241–2259. https://doi.org/10.1016/j.csr.2006.07.016

Aller, R. C., Blair, N. E., Xia, Q., & Rude, P. D. (1996). Remineralization rates, recycling, and storage of carbon in Amazon shelf sediments. *Continental Shelf Research*, *16*(5–6), 753–786. https://doi.org/10.1016/0278-4343(95)00046-1

Allison, M. A., Bianchi, T. S., McKee, B. A., & Sampere, T. P. (2007). Carbon burial on river-dominated continental shelves: Impact of historical changes in sediment loading adjacent to the Mississippi River. *Geophysical Research Letters*, *34*, L01606. https://doi.org/10.1029/2006GL028362

Bao, R., McIntyre, C., Zhao, M., Zhu, C., Kao, S.-J., & Eglinton, T. I. (2016). Widespread dispersal and aging of organic carbon in shallow marginal seas. *Geology*, *44*(10), 791–794. https://doi.org/10.1130/g37948.1

Baudin, F., Martinez, P., Dennielou, B., Charlier, K., Marsset, T., Droz, L., & Rabouille, C. (2017). Organic carbon accumulation in modern sediments of the Angola basin influenced by the Congo deep-sea fan. *Deep-Sea Research Part II*, *142*, 64–74. https://doi.org/10.1016/j.dsr2.2017.01.009

Bauer, J. E., Cai, W.-J., Raymond, P. A., Bianchi, T. S., Hopkinson, C. S., & Regnier, P. A. G. (2013). The changing carbon cycle of the coastal ocean. *Nature*, *504*(7478), 61–70. https://doi.org/10.1038/nature12857

Bender, M. M. (1971). Variations in the $^{13}C/^{12}C$ ratios of plants in relation to the pathway of photosynthetic carbon dioxide fixation. *Phytochemistry*, *10*(6), 1239–1244. https://doi.org/10.1016/s0031-9422(00)84324-1

Berner, R. A. (1982). Burial of organic carbon and pyrite sulfur in the modern ocean: Its geochemical and environmental significance. *American Journal of Science*, *282*(4), 451–473. https://doi.org/10.2475/ajs.282.4.451

Bian, C., Jiang, W., & Greatbatch, R. J. (2013). An exploratory model study of sediment transport sources and deposits in the Bohai Sea, Yellow Sea, and East China Sea. *Journal of Geophysical Research: Oceans*, *118*, 5908–5923. https://doi.org/10.1002/2013jc009116

Bianchi, T. S., & Allison, M. A. (2009). Large-river delta-front estuaries as natural "recorders" of global environmental change. *Proceedings of the National Academy of Sciences of the United States of America*, *106*(20), 8085–8092. https://doi.org/10.1073/pnas.0812878106

Bianchi, T. S., Cui, X., Blair, N. E., Burdige, D. J., Eglinton, T. I., & Galy, V. (2018). Centers of organic carbon burial and oxidation at the land-ocean interface. *Organic Geochemistry*, *115*, 138–155. https://doi.org/10.1016/j.orggeochem.2017.09.008

Bianchi, T. S., Mitra, S., & McKee, B. A. (2002). Sources of terrestrially-derived organic carbon in lower Mississippi River and Louisiana shelf sediments: Implications for differential sedimentation and transport at the coastal margin. *Marine Chemistry*, *77*(2–3), 211–223. https://doi.org/10.1016/s0304-4203(01)00088-3

Blair, N. E., & Aller, R. C. (2012). The fate of terrestrial organic carbon in the marine environment. *Annual Review of Marine Science*, *4*(1), 401–423. https://doi.org/10.1146/annurev-marine-120709-142717

Blair, N. E., Leithold, E. L., Ford, S. T., Peeler, K. A., Holmes, J. C., & Perkey, D. W. (2003). The persistence of memory: The fate of ancient sedimentary organic carbon in a modern sedimentary system. *Geochimica et Cosmochimica Acta*, *67*(1), 63–73. https://doi.org/10.1016/s0016-7037(02)01043-8

Bouillon, S., Connolly, R. M., & Lee, S. Y. (2008). Organic matter exchange and cycling in mangrove ecosystems: Recent insights from stable isotope studies. *Journal of Sea Research*, *59*(1–2), 44–58. https://doi.org/10.1016/j.seares.2007.05.001

Burdige, D. J. (2005). Burial of terrestrial organic matter in marine sediments: A re-assessment. *Global Biogeochemical Cycles*, *19*, GB4011. https://doi.org/10.1029/2004GB002368

Chen, Z., Wu, S., & Xia, D. (1998). *The bay chorography in China (14)*. Beijing, China: Ocean Press.

Coppola, L., Gustafsson, Ö., Andersson, P., Eglinton, T. I., Uchida, M., & Dickens, A. F. (2007). The importance of ultrafine particles as a control on the distribution of organic carbon in Washington Margin and Cascadia Basin sediments. *Chemical Geology*, *243*(1–2), 142–156. https://doi.org/10.1016/j.chemgeo.2007.05.020

Cui, X., Bianchi, T. S., & Savage, C. (2017). Erosion of modern terrestrial organic matter as a major component of sediments in fjords. *Geophysical Research Letters*, *44*, 1457–1465. https://doi.org/10.1002/2016gl072260

de Haas, H., & van Weering, T. C. E. (1997). Recent sediment accumulation, organic carbon burial and transport in the northeastern North Sea. *Marine Geology*, *136*(3–4), 173–187. https://doi.org/10.1016/s0025-3227(96)00072-2

Deng, B., Zhang, J., & Wu, Y. (2006). Recent sediment accumulation and carbon burial in the East China Sea. *Global Biogeochemical Cycles*, *20*, GB3014. https://doi.org/10.1029/2005GB002559

Drenzek, N. J., Montluçon, D. B., Yunker, M. B., Macdonald, R. W., & Eglinton, T. I. (2007). Constraints on the origin of sedimentary organic carbon in the Beaufort Sea from coupled molecular ^{13}C and ^{14}C measurements. *Marine Chemistry*, *103*(1–2), 146–162. https://doi.org/10.1016/j.marchem.2006.06.017

Feng, X., Benitez-Nelson, B. C., Montluçon, D. B., Prahl, F. G., McNichol, A. P., Xu, L., et al. (2013). [14]C and ^{13}C characteristics of higher plant biomarkers in Washington margin surface sediments. *Geochimica et Cosmochimica Acta*, *105*, 14–30. https://doi.org/10.1016/j.gca.2012.11.034

Feng, X., Feakins, S. J., Liu, Z., Ponton, C., Wang, R. Z., Karkabi, E., et al. (2016). Source to sink: Evolution of lignin composition in the Madre de Dios River system with connection to the Amazon basin and offshore. *Journal of Geophysical Research: Biogeosciences*, *121*, 1316–1338. https://doi.org/10.1002/2016jg003323

Fietz, S., Huguet, C., Bendle, J., Escala, M., Gallacher, C., Herfort, L., et al. (2012). Co-variation of crenarchaeol and branched GDGTs in globally-distributed marine and freshwater sedimentary archives. *Global and Planetary Change*, *92–93*, 275–285. https://doi.org/10.1016/j.gloplacha.2012.05.020

Fietz, S., Martínez-Garcia, A., Huguet, C., Rueda, G., & Rosell-Melé, A. (2011). Constraints in the application of the Branched and Isoprenoid Tetraether index as a terrestrial input proxy. *Journal of Geophysical Research*, *116*, C10032. https://doi.org/10.1029/2011JC007062

Fry, B., & Sherr, E. B. (1984). δ^{13}C measurements as indicators of carbon flow in marine and fresh-water ecosystems. *Contributions in Marine Science*, *27*, 13–47.

Galy, V., France-Lanord, C., Beyssac, O., Faure, P., Kudrass, H., & Palhol, F. (2007). Efficient organic carbon burial in the Bengal fan sustained by the Himalayan erosional system. *Nature*, *450*(7168), 407–410. https://doi.org/10.1038/nature06273

Gan, J., Li, L., Wang, D., & Guo, X. (2009). Interaction of a river plume with coastal upwelling in the northeastern South China Sea. *Continental Shelf Research*, *29*(4), 728–740. https://doi.org/10.1016/j.csr.2008.12.002

Goñi, M. A., Hatten, J. A., Wheatcroft, R. A., & Borgeld, J. C. (2013). Particulate organic matter export by two contrasting small mountainous rivers from the Pacific northwest, USA. *Journal of Geophysical Research: Biogeosciences*, *118*, 112–134. https://doi.org/10.1002/jgrg.20024

Goñi, M. A., Monacci, N., Gisewhite, R., Ogston, A., Crockett, J., & Nittrouer, C. (2006). Distribution and sources of particulate organic matter in the water column and sediments of the Fly River Delta, Gulf of Papua (Papua New Guinea). *Estuarine, Coastal and Shelf Science*, *69*(1–2), 225–245. https://doi.org/10.1016/j.ecss.2006.04.012

Goñi, M. A., O'Connor, A. E., Kuzyk, Z. Z., Yunker, M. B., Gobeil, C., & Macdonald, R. W. (2013). Distribution and sources of organic matter in surface marine sediments across the North American Arctic margin. *Journal of Geophysical Research: Oceans*, *118*, 4017–4035. https://doi.org/10.1002/jgrc.20286

Goñi, M. A., Ruttenberg, K. C., & Eglinton, T. I. (1998). A reassessment of the sources and importance of land-derived organic matter in surface sediments from the Gulf of Mexico. *Geochimica et Cosmochimica Acta*, *62*(18), 3055–3075. https://doi.org/10.1016/s0016-7037(98)00217-8

Gordon, E. S., Goñi, M. A., Roberts, Q. N., Kineke, G. C., & Allison, M. A. (2001). Organic matter distribution and accumulation on the inner Louisiana shelf west of the Atchafalaya River. *Continental Shelf Research*, *21*(16–17), 1691–1721. https://doi.org/10.1016/s0278-4343(01)00021-8

Hedges, J. I., Clark, W. A., Quay, P. D., Richey, J. E., Devol, A. H., & Santos, U. D. (1986). Compositions and fluxes of particulate organic material in the Amazon River. *Limnology and Oceanography*, *31*(4), 717–738. https://doi.org/10.4319/lo.1986.31.4.0717

Hedges, J. I., & Keil, R. G. (1995). Sedimentary organic matter preservation: An assessment and speculative synthesis. *Marine Chemistry*, *49*(2-3), 81–115. https://doi.org/10.1016/0304-4203(95)00008-f

Hedges, J. I., & Oades, J. M. (1997). Comparative organic geochemistries of soils and marine sediments. *Organic Geochemistry*, *27*(7–8), 319–361. https://doi.org/10.1016/s0146-6380(97)00056-9

Hilton, R. G., Galy, A., Hovius, N., Horng, M.-J., & Chen, H. (2010). The isotopic composition of particulate organic carbon in mountain rivers of Taiwan. *Geochimica et Cosmochimica Acta*, *74*(11), 3164–3181. https://doi.org/10.1016/j.gca.2010.03.004

Hong, H., Liu, X., Chiang, K.-P., Huang, B., Zhang, C., Hu, J., & Li, Y. (2011). The coupling of temporal and spatial variations of chlorophyll a concentration and the East Asian monsoons in the southern Taiwan Strait. *Continental Shelf Research*, *31*(6), S37–S47. https://doi.org/10.1016/j.csr.2011.02.004

Hopmans, E. C., Weijers, J. W. H., Schefuß, E., Herfort, L., Sinninghe Damsté, J. S., & Schouten, S. (2004). A novel proxy for terrestrial organic matter in sediments based on branched and isoprenoid tetraether lipids. *Earth and Planetary Science Letters*, *224*(1–2), 107–116. https://doi.org/10.1016/j.epsl.2004.05.012

Horng, C.-S., & Huh, C.-A. (2011). Magnetic properties as tracers for source-to-sink dispersal of sediments: A case study in the Taiwan Strait. *Earth and Planetary Science Letters*, *309*(1–2), 141–152. https://doi.org/10.1016/j.epsl.2011.07.002

Hu, B., Li, J., Zhao, J., Wei, H., Yin, X., Li, G., et al. (2014). Late Holocene elemental and isotopic carbon and nitrogen records from the East China Sea inner shelf: Implications for monsoon and upwelling. *Marine Chemistry*, *162*, 60–70. https://doi.org/10.1016/j.marchem.2014.03.008

Hu, J., Hong, H., Li, Y., Jiang, Y., Chen, Z., Zhu, J., et al. (2011). Variable temperature, salinity and water mass structures in the southwestern Taiwan Strait in summer. *Continental Shelf Research*, *31*(6), S13–S23. https://doi.org/10.1016/j.csr.2011.02.003

Hu, J., Kawamura, H., Hong, H., & Pan, W. (2003). A review of research on the upwelling in the Taiwan Strait. *Bulletin of Marine Science*, *73*(3), 605–628.

Hu, J., Kawamura, H., Hong, H., Suetsuga, M., & Lin, M. (2001). Hydrographic and satellite observations of summertime upwelling in the Taiwan Strait: A preliminary description. *Terrestrial, Atmospheric and Oceanic Sciences*, *12*(2), 415–430. https://doi.org/10.3319/tao.2001.12.2.415(o)

Hu, J., Peng, P., Jia, G., Mai, B., & Zhang, G. (2006). Distribution and sources of organic carbon, nitrogen and their isotopes in sediments of the subtropical Pearl River estuary and adjacent shelf, southern China. *Marine Chemistry*, *98*(2–4), 274–285. https://doi.org/10.1016/j.marchem.2005.03.008

Hu, J., & Wang, X. H. (2016). Progress on upwelling studies in the China seas. *Reviews of Geophysics*, *54*(3), 653–673. https://doi.org/10.1002/2015rg000505

Hu, L., Shi, X., Bai, Y., Qiao, S., Li, L., Yu, Y., et al. (2016). Recent organic carbon sequestration in the shelf sediments of the Bohai Sea and Yellow Sea, China. *Journal of Marine Systems*, *155*, 50–58. https://doi.org/10.1016/j.jmarsys.2015.10.018

Hu, L., Shi, X., Yu, Z., Lin, T., Wang, H., Ma, D., et al. (2012). Distribution of sedimentary organic matter in estuarine-inner shelf regions of the East China Sea: Implications for hydrodynamic forces and anthropogenic impact. *Marine Chemistry*, *142-144*, 29–40. https://doi.org/10.1016/j.marchem.2012.08.004

Hu, L. M., Lin, T., Shi, X. F., Yang, Z. S., Wang, H. J., Zhang, G., & Guo, Z. G. (2011). The role of shelf mud depositional process and large river inputs on the fate of organochlorine pesticides in sediments of the Yellow and East China seas. *Geophysical Research Letters*, *38*, L03602. https://doi.org/10.1029/2010GL045723

Huh, C.-A., Chen, W., Hsu, F.-H., Su, C.-C., Chiu, J.-K., Lin, S., et al. (2011). Modern (<100 years) sedimentation in the Taiwan Strait: Rates and source-to-sink pathways elucidated from radionuclides and particle size disttibution. *Continental Shelf Research*, *31*(1), 47–63. https://doi.org/10.1016/j.csr.2010.11.002

Kao, S.-J., Hilton, R. G., Selvaraj, K., Dai, M., Zehetner, F., Huang, J.-C., et al. (2014). Preservation of terrestrial organic carbon in marine sediments offshore Taiwan: Mountain building and atmospheric carbon dioxide sequestration. *Earth Surface Dynamics*, *2*(1), 127–139. https://doi.org/10.5194/esurf-2-127-2014

Kao, S.-J., Jan, S., Hsu, S.-C., Lee, T.-Y., & Dai, M. (2008). Sediment budget in the Taiwan Strait with high fluvial sediment inputs from mountainous rivers: New observations and synthesis. *Terrestrial, Atmospheric and Oceanic Sciences*, *19*(5), 525–546. https://doi.org/10.3319/TAO.2008.19.5.525(Oc)

Kim, J.-H., Schouten, S., Buscail, R., Ludwig, W., Bonnin, J., Sinninghe Damsté, J. S., & Bourrin, F. (2006). Origin and distribution of terrestrial organic matter in the NW Mediterranean (Gulf of Lions): Exploring the newly developed BIT index. *Geochemistry, Geophysics, Geosystems*, *7*, Q11017. https://doi.org/10.1029/2006GC001306

Krishna, M. S., Naidu, S. A., Subbaiah, C. V., Sarma, V. V. S. S., & Reddy, N. P. C. (2013). Distribution and sources of organic matter in surface sediments of the eastern continental margin of India. *Journal of Geophysical Research: Biogeosciences*, *118*, 1484–1494. https://doi.org/10.1002/2013jg002424

Li, X., Bianchi, T. S., Allison, M. A., Chapman, P., & Yang, G. (2013). Historical reconstruction of organic carbon decay and preservation in sediments on the East China Sea shelf. *Journal of Geophysical Research: Biogeosciences*, *118*, 1079–1093. https://doi.org/10.1002/jgrg.20079

Liang, W. D., Tang, T. Y., Yang, Y. J., Ko, M. T., & Chuang, W. S. (2003). Upper-ocean currents around Taiwan. *Deep-Sea Research Part II*, *50*(6–7), 1085–1105. https://doi.org/10.1016/s0967-0645(03)00011-0

Lin, H., Cai, Y., Sun, X., Chen, G., Huang, B., Cheng, H., & Chen, M. (2016). Sources and mixing behavior of chromophoric dissolved organic matter in the Taiwan Strait. *Marine Chemistry*, *187*, 43–56. https://doi.org/10.1016/j.marchem.2016.11.001

Liu, J. P., Li, A. C., Xu, K. H., Veiozzi, D. M., Yang, Z. S., Milliman, J. D., & DeMaster, D. J. (2006). Sedimentary features of the Yangtze River-derived along-shelf clinoform deposit in the East China Sea. *Continental Shelf Research*, *26*(17–18), 2141–2156. https://doi.org/10.1016/j.csr.2006.07.013

Liu, J. P., Xu, K. H., Li, A. C., Milliman, J. D., Velozzi, D. M., Xiao, S. B., & Yang, Z. S. (2007). Flux and fate of Yangtze river sediment delivered to the East China Sea. *Geomorphology*, *85*(3–4), 208–224. https://doi.org/10.1016/j.geomorph.2006.03.023

Meyers, P. A. (1994). Preservation of elemental and isotopic source identification of sedimentary organic-matter. *Chemical Geology*, *114*(3–4), 289–302. https://doi.org/10.1016/0009-2541(94)90059-0

Meyers, P. A. (1997). Organic geochemical proxies of paleoceanographic, paleolimnologic, and paleoclimatic processes. *Organic Geochemistry*, *27*(5–6), 213–250. https://doi.org/10.1016/s0146-6380(97)00049-1

Milliman, J. D., & Farnsworth, K. L. (2011). *River discharge to the coastal ocean: A global synthesis*. Cambridge, UK: Cambridge University Press. https://doi.org/10.1017/CBO9780511781247

Pearson, E. J., Juggins, S., Talbot, H. M., Weckström, J., Rosén, P., Ryves, D. B., et al. (2011). A lacustrine GDGT-temperature calibration from the Scandinavian Arctic to Antarctic: Renewed potential for the application of GDGT-paleothermometry in lakes. *Geochimica et Cosmochimica Acta*, *75*(20), 6225–6238. https://doi.org/10.1016/j.gca.2011.07.042

Qiu, Y., Li, L., Chen, C.-T. A., Guo, X., & Jing, C. (2011). Currents in the Taiwan Strait as observed by surface drifters. *Journal of Oceanography*, *67*(4), 395–404. https://doi.org/10.1007/s10872-011-0033-4

Ramaswamy, V., Gaye, B., Shirodkar, P. V., Rao, P. S., Chivas, A. R., Wheeler, D., & Thwin, S. (2008). Distribution and sources of organic carbon, nitrogen and their isotopic signatures in sediments from the Ayeyarwady (Irrawaddy) continental shelf, northern Andaman Sea. *Marine Chemistry*, *111*(3–4), 137–150. https://doi.org/10.1016/j.marchem.2008.04.006

Schouten, S., Forster, A., Panoto, F. E., & Sinninghe Damsté, J. S. (2007). Towards calibration of the TEX$_{86}$ palaeothermometer for tropical sea surface temperatures in ancient greenhouse worlds. *Organic Geochemistry*, *38*(9), 1537–1546. https://doi.org/10.1016/j.orggeochem.2007.05.014

Schreiner, K. M., Bianchi, T. S., Eglinton, T. I., Allison, M. A., & Hanna, A. J. M. (2013). Sources of terrigenous inputs to surface sediments of the Colville River Delta and Simpson's Lagoon, Beaufort Sea, Alaska. *Journal of Geophysical Research: Biogeosciences*, *118*, 808–824. https://doi.org/10.1002/jgrg.20065

Shang, S. L., Zhang, C. Y., Hong, H. S., Shang, S. P., & Chai, F. (2004). Short-term variability of chlorophyll associated with upwelling events in the Taiwan Strait during the southwest monsoon of 1998. *Deep-Sea Research Part II*, *51*(10–11), 1113–1127. https://doi.org/10.1016/j.dsr2.2004.04.003

Smith, R. W., Bianchi, T. S., & Li, X. (2012). A re-evaluation of the use of branched GDGTs as terrestrial biomarkers: Implications for the BIT index. *Geochimica et Cosmochimica Acta*, *80*, 14–29. https://doi.org/10.1016/j.gca.2011.11.025

Smith, R. W., Bianchi, T. S., & Savage, C. (2010). Comparison of lignin phenols and branched/isoprenoid tetraethers (BIT index) as indices of terrestrial organic matter in Doubtful Sound, Fiordland, New Zealand. *Organic Geochemistry*, *41*(3), 281–290. https://doi.org/10.1016/j.orggeochem.2009.10.009

Stallard, R. F. (1998). Terrestrial sedimentation and the carbon cycle: Coupling weathering and erosion to carbon burial. *Global Biogeochemical Cycles*, *12*(2), 231–257. https://doi.org/10.1029/98GB00741

Sun, D., Tang, J., He, Y., Liao, W., & Sun, Y. (2018). Sources, distributions, and burial efficiency of terrigenous organic matter in surface sediments from the Yellow River mouth, northeast China. *Organic Geochemistry*, *118*, 89–102. https://doi.org/10.1016/j.orggeochem.2017.12.009

Sun, X., Lin, C., Huang, H., Zhang, Y., Lin, H., & Ji, W. (2012). Distribution of total organic carbon contents and inflencing factors in Taiwan Strait and adjacent waters in summer (in Chinese with English abstract). *Journal of Oceanography in Taiwan Strait*, *31*(1), 12–19.

Tang, D. L., Kester, D. R., Ni, I.-H., Kawamura, H., & Hong, H. (2002). Upwelling in the Taiwan Strait during the summer monsoon detected by satellite and shipboard measurements. *Remote Sensing of Environment*, *83*(3), 457–471. https://doi.org/10.1016/s0034-4257(02)00062-7

Tao, S., Eglinton, T. I., Montluçon, D. B., McIntyre, C., & Zhao, M. (2015). Pre-aged soil organic carbon as a major component of the Yellow River suspended load: Regional significance and global relevance. *Earth and Planetary Science Letters*, *414*, 77–86. https://doi.org/10.1016/j.epsl.2015.01.004

Walsh, E. M., Ingalls, A. E., & Keil, R. G. (2008). Sources and transport of terrestrial organic matter in Vancouver Island fjords and the Vancouver-Washington Margin: A multiproxy approach using $\delta^{13}C_{org}$, lignin phenols, and the ether lipid BIT index. *Limnology and Oceanography*, *53*(3), 1054–1063. https://doi.org/10.4319/lo.2008.53.3.1054

Wang, A.-J., Ye, X., Liu, J. T., Xu, Y.-H., Yin, X.-J., & Xu, X.-H. (2017). Sources of settling particulate organic carbon during summer in the northern Taiwan Strait. *Estuarine, Coastal and Shelf Science*, *198*, 487–496. https://doi.org/10.1016/j.ecss.2016.10.008

Wang, D., Zheng, Q., & Hu, J. (2013). Jet-like features of Jiulongjiang River plume discharging into the west Taiwan Strait. *Frontiers of Earth Science*, *7*(3), 282–294. https://doi.org/10.1007/s11707-013-0372-0

Weijers, J. W. H., Schouten, S., Schefuß, E., Schneider, R. R., & Sinninghe Damsté, J. S. (2009). Disentangling marine, soil and plant organic carbon contributions to continental margin sediments: A multi-proxy approach in a 20,000 year sediment record from the Congo deep-sea fan. *Geochimica et Cosmochimica Acta*, *73*(1), 119–132. https://doi.org/10.1016/j.gca.2008.10.016

Weijers, J. W. H., Schouten, S., Spaargaren, O. C., & Sinninghe Damsté, J. S. (2006). Occurrence and distribution of tetraether membrane lipids in soils: Implications for the use of the TEX_{86} proxy and the BIT index. *Organic Geochemistry*, *37*(12), 1680–1693. https://doi.org/10.1016/j.orggeochem.2006.07.018

Wu, Y., Bao, H., Yu, H., Zhang, J., & Kattner, G. (2015). Temporal variability of particulate organic carbon in the lower Changjiang (Yangtze River) in the post-Three Gorges Dam period: Links to anthropogenic and climate impacts. *Journal of Geophysical Research: Biogeosciences*, *120*, 2194–2211. https://doi.org/10.1002/2015jg002927

Wu, Y., Eglinton, T., Yang, L., Deng, B., Montluçon, D., & Zhang, J. (2013). Spatial variability in the abundance, composition, and age of organic matter in surficial sediments of the East China Sea. *Journal of Geophysical Research: Biogeosciences*, *118*, 1495–1507. https://doi.org/10.1002/2013jg002286

Wu, Y., Zhang, J., Liu, S. M., Zhang, Z. F., Yao, Q. Z., Hong, G. H., & Cooper, L. (2007). Sources and distribution of carbon within the Yangtze River system. *Estuarine, Coastal and Shelf Science*, *71*(1–2), 13–25. https://doi.org/10.1016/j.ecss.2006.08.016

Xing, L., Hou, D., Wang, X., Li, L., & Zhao, M. (2016). Assessment of the sources of sedimentary organic matter in the Bohai Sea and the northern Yellow Sea using biomarker proxies. *Estuarine, Coastal and Shelf Science*, *176*, 67–75. https://doi.org/10.1016/j.ecss.2016.04.009

Xing, L., Zhao, M., Gao, W., Wang, F., Zhang, H., Li, L., et al. (2014). Multiple proxy estimates of source and spatial variation in organic matter in surface sediments from the southern Yellow Sea. *Organic Geochemistry*, *76*, 72–81. https://doi.org/10.1016/j.orggeochem.2014.07.005

Yang, H., Lü, X., Ding, W., Lei, Y., Dang, X., & Xie, S. (2015). The 6-methyl branched tetraethers significantly affect the performance of the methylation index (MBT') in soils from an altitudinal transect at Mount Shennongjia. *Organic Geochemistry*, *82*, 42–53. https://doi.org/10.1016/j.orggeochem.2015.02.003

Yao, P., Yu, Z., Bianchi, T. S., Guo, Z., Zhao, M., Knappy, C. S., et al. (2015). A multiproxy analysis of sedimentary organic carbon in the Changjiang Estuary and adjacent shelf. *Journal of Geophysical Research: Biogeosciences*, *120*, 1407–1429. https://doi.org/10.1002/2014jg002831

Zhang, J., Wu, Y., Jennejahn, T. C., Ittekkot, V., & He, Q. (2007). Distribution of organic matter in the Changjiang (Yangtze River) Estuary and their stable carbon and nitrogen isotopic ratios: Implications for source discrimination and sedimentary dynamics. *Marine Chemistry*, *106*(1–2), 111–126. https://doi.org/10.1016/j.marchem.2007.02.003

Zhu, C., Wagner, T., Pan, J.-M., & Pancost, R. D. (2011). Multiple sources and extensive degradation of terrestrial sedimentary organic matter across an energetic, wide continental shelf. *Geochemistry, Geophysics, Geosystems*, *12*, Q08011. https://doi.org/10.1029/2011GC003506

Zhu, C., Wagner, T., Talbot, H. M., Weijers, J. W. H., Pan, J.-M., & Pancost, R. D. (2013). Mechanistic controls on diverse fates of terrestrial organic components in the East China Sea. *Geochimica et Cosmochimica Acta*, *117*, 129–143. https://doi.org/10.1016/j.gca.2013.04.015